coatings

MDPI

Article

Preparation and Characterization of Stable Superhydrophobic Copper Foams Suitable for Treatment of Oily Wastewater

Aikaterini Baxevani [1], Fani Stergioudi [1,*], Nikolaos Patsatzis [1], Lamprini Malletzidou [2], George Vourlias [2] and Stefanos Skolianos [1]

[1] Physical Metallurgy Laboratory, School of Mechanical Engineering, Aristotle University of Thessaloniki, GR-54124 Thessaloniki, Greece
[2] Laboratory of Advanced Materials & Devices, School of Physics, Faculty of Sciences, Aristotle University of Thessaloniki, GR-54124 Thessaloniki, Greece
* Correspondence: fstergio@auth.gr

Abstract: A simple two-stage chemical solution process is reported, to deposit a superhydrophobic film on copper foams with a view to be employed in oil absorption or filtration procedures. The first stage includes the growth of a silver layer to increase micro roughness and the second one evolves the modification of the film using stearic acid. The whole process is time-saving, cost effective and versatile. UV-Vis spectroscopy was employed to determine optimum deposition durations and detect potential film detachments during the synthesis process. Scanning electron microscopy (SEM) and energy dispersive spectroscopy (EDS) were used to examine the film structure and elemental analysis. Surface functional groups were detected by Fourier transform infrared (FTIR) spectroscopy. An adherent superhydrophobic silver coating was achieved under optimum deposition durations. A leaf-like structural morphology appeared from silver deposition and spherical, microflower morphologies stemmed from the stearic acid deposition. The influence of process conditions on wettability and the obtained silver film morphology and topography were clarified. Thermal stability at several temperatures along with chemical stability for acidic and alkaline environments were examined. Oil absorption capacity and separation efficiency were also evaluated for the optimum superhydrophobic copper foams. The results showed that the produced superhydrophobic copper foams can potentially be used to oil/water separation applications.

Keywords: superhydrophobicity; copper foam; durability; stability; nanostructure

Citation: Baxevani, A.; Stergioudi, F.; Patsatzis, N.; Malletzidou, L.; Vourlias, G.; Skolianos, S. Preparation and Characterization of Stable Superhydrophobic Copper Foams Suitable for Treatment of Oily Wastewater. *Coatings* **2023**, *13*, 355. https://doi.org/10.3390/coatings13020355

Academic Editor: Robert J. K. Wood

Received: 19 December 2022
Revised: 19 January 2023
Accepted: 28 January 2023
Published: 3 February 2023

1. Introduction

Industrialization and economic development have caused an increase in water pollution such as oil spills, oily wastewater discharge and oil diffusion during drilling. Traditional methods and technologies are utilized to separate oil from water, including adsorption, degradation, oil skimmers, coalescence, flocculation, flotation gravity separation, centrifuge, sedimentation and hydrocyclone separation [1–4]. These methods are time-consuming, energy intensive, low efficiency and suffer from high operation cost. It is crucial to develop a facile, cost-effective and time-saving method for oil/water separation applications. Superhydrophobic surfaces are bioinspired (e.g., from lotus leaf, shark skin, strider leg) and their wettability was evaluated using static water contact angle (WCA) measurements [5–7].

In the last decades, metal foams have attracted the interest of the scientific community. Many research works focused on methods and processes of developing superhydrophobic surfaces on metallic foams to examine their special characteristics and related applications fields. Potential application fields are related with the high repellency of the water such as anti-icing, anti-fogging, anti-corrosion and self-cleaning surface technologies [8–18]. Superhydrophobic surfaces production mainly includes two important approaches: to

increase the substrate's micro/nano roughness and to decrease surface energy [19–22]. Notwithstanding, the various methods of growing superhydrophobic surfaces reported in the literature, durability of the hydrophobic films still remains a challenge. Numerous production techniques reported in the literature suffer certain drawbacks, such as multiple and complex stages, highly cost materials and equipment, or time consuming processes.

Nickel foams coated with $ZnO@Co_3O_4$ hierarchical structure showed excellent abrasion resistance, chemical stability and high oil/water separation efficiency [23]. Modified nickel foams with a mixture of polytetratluoroethylene (PTFE) and hydrophobic fumed silica exhibited a WCA of 155° and high separation efficiency above 96% for the more viscous olive oil/water mixture and above 99% for the hexane/water mixture [24]. Hydrophobic aluminum foams were developed via immersion in NaOH solution and in an ethanolic solution of dodecanoic acid for 2 h. The achieved water contact angle was 122° and separation efficiencies up to 94.91% [25]. Tang et al. [26] developed a superhydrophilic membrane using tannic acid (TA), polyvinylpyrrolidone (PVP) and hydrophilic silicon dioxide particles (SiO_2). TA solution was added into PVP solution dropwise and stirred strongly for 2.5 h. After that, so as to form a gel, SiO_2 was added into the mixture. The colloidal solution was poured into a filtration cell under a negative pressure of −0.09 MPa. This process is long lasting and special conditions are needed. Zeng et al. [27] produced a novel Janus sponge by modifying one side of a PA@PEI-sponge with PDMS. PA@PEI-sponge is a superhydrophilic sponge and was prepared via synthesizing negatively-charged phytic acid@polyethyleneimine (PA@PEI) nanoparticles and assembling them on the surface of polydopamine (PDA) and PEI-modified polyurethane (PU) sponge through electrostatic adsorption. This procedure has complex and multiple stages. A superhydrophobic Fe foam was prepared by Liu et al. [28] via an immersion method with cupric chloride and stearic acid plus a heat treatment in a furnace at 250 °C for 2 h and achieved WCA of 157°. A long lasting and energy consuming method was used again in order to develop a hydrophobic surface. Zhang et al. [29] developed coated copper meshes via an immersion in a mixed alkaline solution with NaOH and $(NH_4)2S_2O_8$. WCA of approximately 153° was achieved, a value which is similar to previous ones.

Among metal foams, copper foams have attracted huge attention due to their large specific area, high electrical, along with thermal, conductivity and ductility. Modification methods of copper foam include sol–gel, plasma spray, spin coating and electrospinning, techniques which suffer certain drawbacks, such as complexity, use of environmentally harmful solvents, high energy consumption [12,14,17,30–32].

Xu et al. [33] produced superhydrophobic copper foams with a solution-immersion process. Copper substrates were immersed in ethanolic stearic acid solution for 4 days and achieved WCA was 156°. Wang et al. [34] fabricated superhydrophobic copper sheets with template deposition method. After the preparation of polystyrene microspheres powders, copper plate was put in polystyrene colloidal microspheres with $CuSO_4$ solution as an electrolyte. At the end of procedure, the surface was modified using fluorosilane solution and the achieved WCA was 156.3°. The aforementioned long-lasting procedures have complex and multiple stages. Bhagat and Gupta [35] developed micro-texturing superhydrophobic silicon wafers by high power laser. These microstructures were thermally replicated on a polycarbonate surface by putting them between two hot plates with different temperatures. Maximum achieved WCA was 155°. In this procedure, there is use of high-cost equipment and there is a need of high amounts of electric power. Copper metal foams were transitioned from superhydrophilic to hydrophobic by Shirazy et al. [36]. They used a hydrogen reduction process with a gas mixture of 7% hydrogen plus 93% nitrogen and a heating process from room temperature (∼20 °C) to 600 °C in 2 h, which was followed by a 2 h plateau at 600 °C. In this process, there is a use of high amounts of energy so as to reach 600 °C, and the use of gases, which are factors that increase the difficulty and the cost of the process.

It is clear that there is a major interest for hydrophobic surfaces and a plethora of research works focused on this field. The most challenging factor is to achieve a WCA higher

than 160°. The majority of research works achieve WCAs between 150° and 155°. It was crucial to combine the simplicity of the process with a WCA higher than the achieved values of contact angles in the most studies. In this study, there are only two short-term stages. Additionally, the need for limited amounts of the raw materials renders the production process as cost effective. The achievement of a WCA of 180° is significant, combined with the stability of the coating. Absorption spectra of the solutions were obtained, through UV-Visible spectroscopy experiments. The use of UV-Vis spectroscopy was considered of great importance, to ensure the optimum intervals of immersion and optimize the process so as to achieve a WCA of 180°. Nitrate ions concentration was calculated by Lambert–Beer law [37]. The proposed approach for preparing superhydrophobic copper foams offers simplicity and, therefore, ease of commercialization with promising contribution in treatment of oily wastewater.

2. Materials and Methods

2.1. Materials

Silver nitrate was purchased from Panreac (Barcelona, Spain) and stearic acid ($C_{18}H_{36}O_2$) was a product of Merck (Darmstadt, Germany). Copper metal foams, that were used in this study, have a mean pore size of 1.6 mm, 93.6% porosity and are in the form of 10 cm × 10 cm × 0.3 cm sheets and were provided by Metafoam Technologies (Brossard, Canada). Ethanol was purchased from Central-chem (Bratislava, Slovakia). Sodium hydroxide (NaOH) and hydrochloric acid (HCl), used in chemical stability tests, are products of Honeywell (Seelze, Germany) and Panreac (Barcelona, Spain), respectively.

2.2. Preparation of Superhydrophobic Copper Foams

Copper foam sheets (15 mm × 15 mm × 2 mm) were ultrasonically cleaned with acetone and anhydrous ethanol for 5 min, three times alternately. The process of growing a superhydrophobic coating includes two stages as illustrated in Figure 1. The pretreated copper foam sheets were immersed in a 20 mM silver nitrate ($AgNO_3$) ethanolic solution at 50 °C, to increase foams' micro/nano-roughness and subsequently in a 15 mM stearic acid ethanolic solution to reduce its surface-energy. This two-stage process was recurrent for 20 and 30 min immersion times in silver nitrate solution and for 20, 30, 40, 50 and 60 min in stearic acid solution. Finally, the produced coated copper foams were washed with deionized water and dried at room temperature. It should be mentioned that small quantities of both chemical compounds were used. Specifically, 0.17 g of silver nitrate and 0.21 g of stearic acid are sufficient quantities to coat four samples of copper foam sheets. Therefore, the use of silver nitrate does induce a considerable cost increase in the production process.

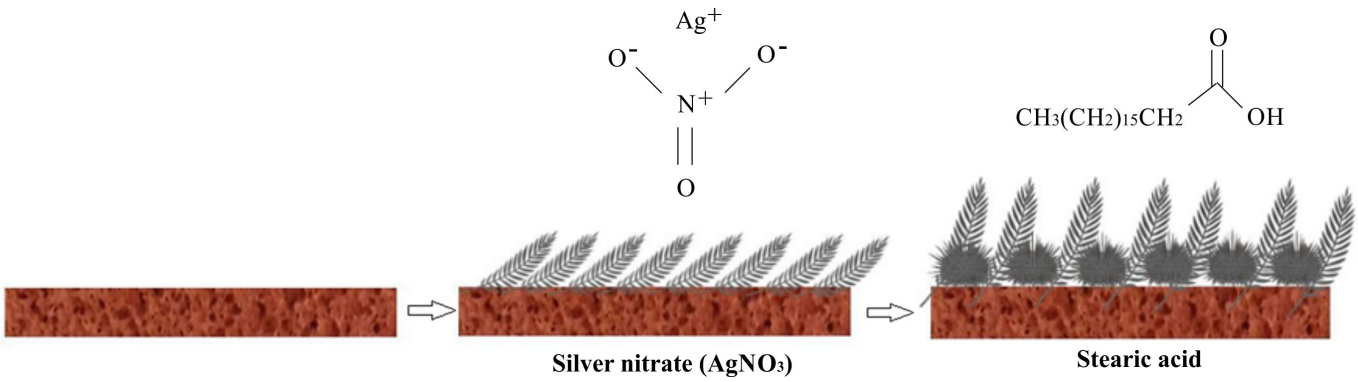

Figure 1. Schematic illustration of superhydrophobic copper foam production stages.

2.3. Characterization of Superhydrophobic Copper Foam

Static water contact angle (WCA) was used to evaluate surface wettability by employing 6 μL water droplets. UV-Vis spectroscopy experiments (using a UV-1800 spec-

trophotometer, Shimadzu, Tokyo, Japan) were conducted, aiming to take absorption spectra of silver nitrate solution and optimize the duration of this immersion stage. Samples were taken at specific time intervals from the silver nitrate solutions. Scanning electron microscopy (Phenom ProX desktop SEM, Thermo Fisher Scientific, Eindhoven, The Netherlands) equipped with an energy dispersive spectrometer EDS was used to characterize the microstructure and the phases developed in the produced superhydrophobic films. Surface functional groups of the developed superhydrophobic film were evaluated by Fourier transform infrared (FTIR) spectroscopy, with a Cary 670 spectroscope (Agilent Technologies, Palo Alto, CA, USA), in attenuated total reflectance (ATR) mode, using a diamond ATR device, model GladiATR (Pike Technologies, Madison, WI, USA). The spectra were collected in the Mid-IR region, with 32 scans and a resolution of 4 cm^{-1}. The chemical stability of the superhydrophobic copper foam was identified by the effects of different acids and alkali solutions with pH ranging from 1 to 13. More specifically, the superhydrophobic copper foam sheets (15 mm × 15 mm × 2 mm) were immersed in aqueous solutions of HCl (10 wt%) and NaOH (10 wt%) for 1 h and 3 h, respectively. Thermal stability was checked for −15 and 100 °C for 1, 3 and 24 h using a laboratory incubator (CLIMACELL incubator, MMM Group, Munich, Germany). Each test was repeated at least three times. Reduction of surface's hydrophobicity after these treatments was measured via WCA. Each WCA value came as a mean value of 3 measurements.

The absorption capacity was calculated through the Equation (1)

$$\frac{w_1 - w_2}{w_1} \quad (1)$$

where w_1 is the weight of the foam before the absorption and w_2 is the weight of the foam after the absorption.

The separation efficiency (s) is calculated as (M_2/M_1) where M_1 is the weight of water added before separation and M_2 is the weight of water collected in the filtrate tank after separation.

3. Results and Discussion

3.1. Effect of Immersion Time

Immersion time in the process stages plays a vital role in foams' modification. Surfaces' micro-roughness and energy reduction are determining factors for developing hydrophobic coatings on metal foams and they are directly linked to immersion time [38,39]. UV-Vis spectroscopy was used to estimate the optimum immersion duration in the silver nitrate solution. UV-Vis absorption spectra of silver nitrate solution were obtained at specific time intervals so as to differentiate the precipitation of silver on copper metallic foam. An indicative absorption spectrum (out of 23 in total) is shown in Figure 2a. The peak at around 308 nm corresponds to the nitrate anions [40], while the peak at 224 nm to the silver cations [41], which appeared from the dissolution of silver nitrate in ethanol. At the highest peak, the absorptions are due to combination with the solvent (ethanol), so it is more difficult to obtain clear results for increasing or decreasing of the Ag^+ concentration. Thus, the absorption of nitrate ions was taken by regular sampling over a period of 30 min and its diagram is depicted in Figure 2b. The corresponding change in their concentration is shown in Figure 2c. The concentration was calculated by the Lambert–Beer law (Equation (2)), with a molecular absorption coefficient which was calculated from the first sample (5.6 $M^{-1}cm^{-1}$), where both the absorption and the concentration of nitrate ions were known.

$$A = \alpha_\lambda * b * c \quad (2)$$

where A is the absorbance; α_λ is the molar attenuation coefficient or absorptivity of the attenuating species; b is the optical path length in cm; c is the concentration of the attenuating species.

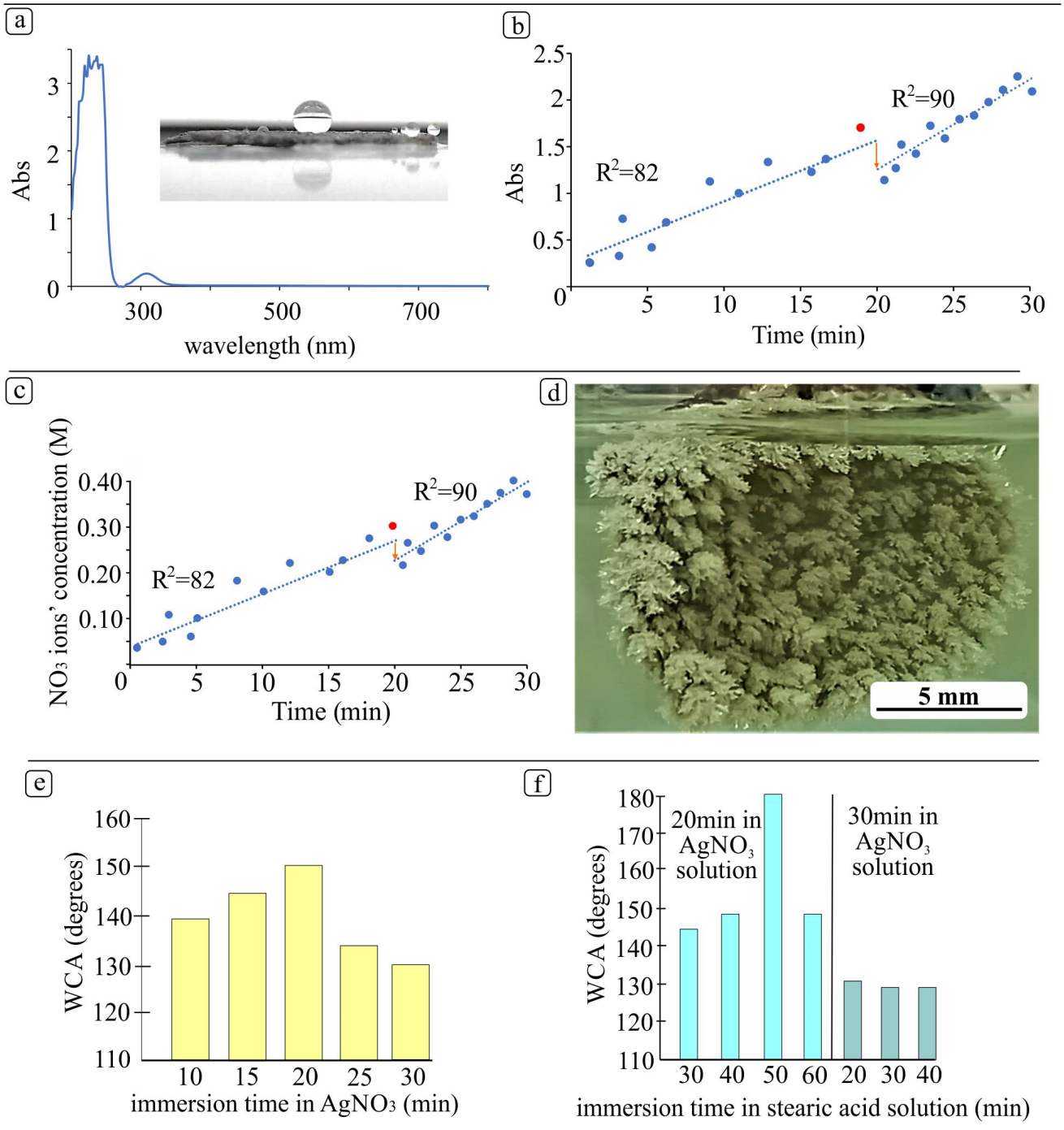

Figure 2. (**a**) Indicative UV-vis absorption spectrum, (**b**) nitrate ions' absorbance as a function of time, (**c**) nitrate ions' concentration as a function of time, (**d**) development of silver coating on the copper foam substrate, (**e**) WCA measurements for different minutes of immersion time in $AgNO_3$, (**f**) WCA's measurements for 20 min and 30 min of immersion time in $AgNO_3$ solution as a function of various immersion times in stearic acid solution.

The concentration of nitrate ions changes incrementally with time for the first 21 min of precipitation. This increase is almost linear, as the experimental data fluctuate around an average value, which is represented by the trend line (R^2 = 82). The increase in the concentration of NO_3^- over time is justified by the fact that over time the metal foam is coated with silver and, as a result, the amount of silver cations decreases and the amount

of nitrates remains constant (since they do not participate in reaction), thus leading to increasing the concentration of the latter, due to the maintenance of the volume of the solution and due to the existence of stoichiometry. However, the nitrate concentration at 21 min decreased sharply (marked with red arrows in Figure 2b,c), which indicates that there is a silver detachment from the surface of copper foam (from one point onwards), which means that although the coating process still takes place, several layers of silver (multilayer coating) must have been created on the surface of the copper. The trend line also changes after 21 min, remaining almost linear, with different slope and with R^2 = 90). Silver coating consists of successive layers, which indicates that at the outer layers, the adhesion of the coating diminishes. Figure 2d depicts the development of Ag microstructure on copper substrate. Leaf-like microstructural layers covered completely the surface of the copper foam. However, the outer deposited layers on the leaf-like morphologies created weaker bonds, especially in the time interval between 20 and 30 min, where they detach easily. This was also attested by the WCA measurements (Figure 2e), where a superficial detachment of the outer layers formation was observed in the water droplets. Thus, the optimal precipitation time is considered to be 20 min due to the sharp reduction of the nitrate ions concentration at 21 min, even though there is an increase after 21 min. UV-vis spectra are of great importance, because they warrant and confirm that the immersion time of 20 min in silver nitrate solution, leads to the highest absorbance and NO_3^- concentration, thus leading to the optimum silver deposition time.

When immersion time in $AgNO_3$ solution was higher than 30 min, lack of adhesion for the coating was observed, resulting in its degradation. The adhesion of the coating was examined through dropping water droplets on the surface. In some cases (e.g., when immersion time in $AgNO_3$ solution was 30 min), when a droplet rolled off the surface, it drifted away part of the coating that was subsequently incorporated into the water droplet. This observation led to the conclusion that there is a partial detachment of the coating and lack of adhesion. WCA measurements were about 130° for various immersion time intervals of 20, 30 and 40 min in stearic acid solution (Figure 2f), an indication that confirms the previous observation.

UV-Vis spectroscopy could not be used for optimizing the immersion time in the stearic acid solution since it absorbs in the IR and not in the ultraviolet-visible spectral region. Figure 2f also depicts WCA for the optimum 20 min of immersion in silver nitrate solution and for several immersion time intervals of 30, 40, 50 and 60 min in stearic acid solution. The highest WCA was achieved for 20 min of immersion in silver nitrate solution and for 50 min in stearic acid solution. WCA's measurements for 20 min of immersion in silver nitrate solution and for 30, 40 and 60 min in stearic acid solution, was about 145°, respectively. WCA reached the optimum 180° when immersion time in silver nitrate solution is 20 min and in stearic acid solution is 50 min. Therefore, the optimum immersion duration in the stearic acid solution was set to 50 min.

To identify the chemical bonds of the system and confirm the presence of the stearic acid, ATR-FTIR measurements were conducted for the superhydrophobic copper foam sample prepared under the optimum conditions. Figure 3 shows the ATR-FTIR spectra of stearic acid (solid) and stearic copper surface after modification, for comparative reasons. The results exhibit the presence of stearate together with that of stearic acid because of the C-H bands at 3000–2800 cm^{-1}, at 1698 cm^{-1} (-COOH) and at 720 cm^{-1} (-CH_2) [42–45]. However, the emergence of a band at 1585 cm^{-1} indicates the formation of copper stearate. The concurrent presence of silver stearate cannot be excluded, because of two bands of low intensity (inset of Figure 3) at 1512 and 1420 cm^{-1}, which correspond to -COO^- asymmetric and symmetric stretching, respectively.

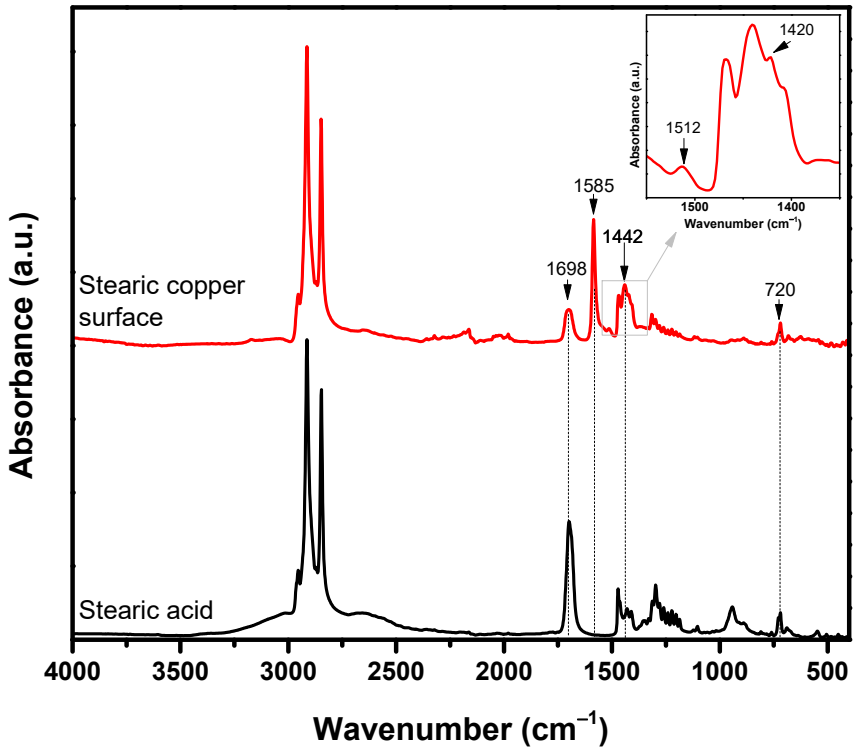

Figure 3. ATR-FTIR spectra of stearic acid and stearic copper surface after modification. The inset presents the region of interest regarding the presence of silver stearate in the spectrum of stearic copper surface.

Higher magnification SEM images of the modified copper foam prepared under optimum conditions (shown in Figure 4) clearly revealed two different morphologies on the surface. The leaf-like nanorods and highly branched dendrites correspond to Ag morphologies (Figure 4a,b). These fractal-like structures are composed of many self-assembled polygonals which were identified by EDS analyses as silver. In Figure 4a, a two-tier roughness is revealed, on a larger scale, e.g., a micro-roughness stemming from the leaf morphologies and a nano-roughness (indicated by arrows) on the surface of these leaf/dendritic morphologies as shown in Figure 4a. Similar leaf-like and dendritic morphologies are well documented in literature [46,47]. The above results are in accordance with the literature which reports that the formation of silver superhydrophobic nanocoatings follows a process of initial reduction, nucleation, adsorption, growth, branching, and further growth [46–48]. Developed morphologies of the silver film depend on the Ag^+ reaction time and the strength of the reducing agent(s) in the system. Leaf like morphologies are favored in low strength reducing agent, which in our case is the copper foam substrate [48].

The spherical micro-clusters of flower-like morphologies correspond to copper stearate nanostructures (Figure 4c). It was observed that the flower-like morphologies arise from the copper substrate that was not fully covered with the Ag^+ ions in the previous production step and are in the form of nanosheets that are entangled with each other (Figure 4c).

The acidic environment of the ethanolic stearic acid solution oxides the copper and releases Cu^{2+} ions which are then captured by the stearic acid and precipitate as copper stearate, as confirmed by FTIR analysis, in the form of nanosheets. Possible occurring reaction is shown in Equation (3) [49]:

$$Cu^{2+} + 2CH_3(CH_2)_{16}COOH \rightarrow Cu[CH_3(CH_2)_{16}COO]_2 + 2H^+ \quad (3)$$

Figure 5 depicts SEM images of hydrophobic coated copper foams produced at different immersion times in stearic acid solution. Figure 5a shows the morphology of the initial copper foam substrate before the growth of silver coating, for reasons of compari-

son. Figure 5b,c show the coating's morphology for 20 min of immersion in silver nitrate solution and 40 min in stearic acid solution. Fractal-structure morphologies of the film are not developed completely. Few small sized stems, branches and leaf-like structures are depicted. Figure 5d–f depict surface morphology of the optimum coated copper foam which reacted in silver nitrate solution for 20 min and in stearic acid solution for 50 min. Leaf-like and micro-flower structures are completely developed. It is clear that micro-nano hierarchical dendritic structures and nanoribbons are fully developed, which is also consistent with the WCA measurements that demonstrate a super-hydrophobic behavior of this sample. Figure 5g–i depict the microstructure which corresponds to 20 min of immersion in silver nitrate solution and 60 min of immersion in stearic acid solution. Spherical microclusters of flower-like morphology prevail, which indicates the presence of copper stearate; however, it seems that the silver leaf-like morphology was affected and was hardly visible in SEM images. This is probably ascribed to the extending coverage of the copper substrate with the flower-like copper stearate morphologies that either cover the original silver leaf morphologies or destroy them during the stacking of the nanosheets of the copper stearate. Similar behavior was observed in [49] where the copper stearate morphologies prevailed over all other formed nanostructures when the immersion time was increased.

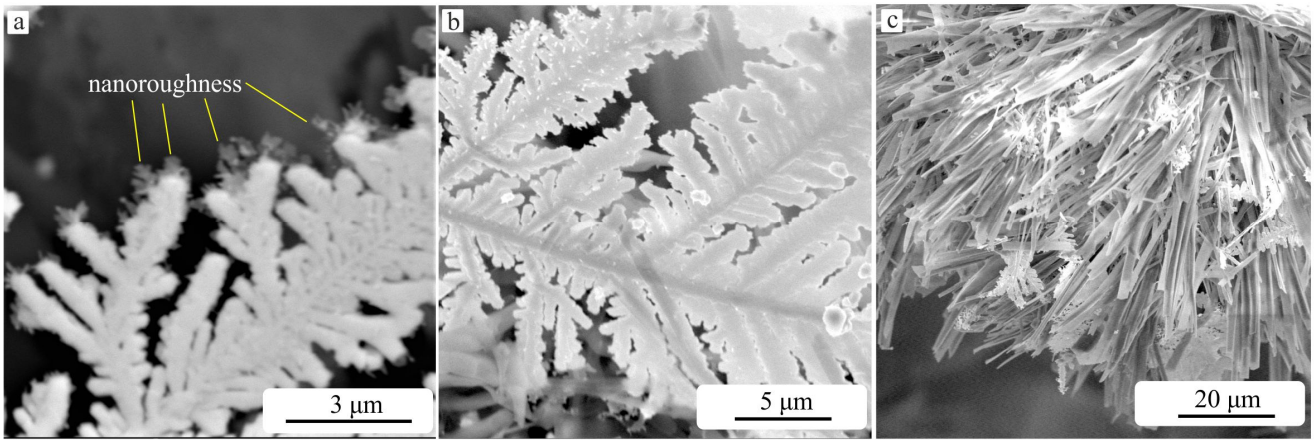

Figure 4. High magnification SEM images of the two different morphologies developed on the superhydrophobic copper foam. (**a**,**b**) for the silver and (**c**) for the copper stearate.

3.2. Surface Wettability

Figure 6a–c depicts oil and water droplets on the copper foam's surface. It is discernible that water droplets have a spherical shape due to the formation of a continuous air gap between water and superhydrophobic surface, leading to a non-wetting behavior (Cassie-Baxter phenomenon). Oil droplets of the same volume permeated through the foam indicating the surface's oleophilicity [50].

To assess the superhydrophobic copper foam wettability, a dynamic rolling test was performed without giving any inclination to the sample. The water droplets were immediately rolling away from the copper foam surface as depicted in the Supplementary Video S1. The short contact time between water droplets and modified copper foam confirms the surface's high water resistivity [18,51]. Continuous needle flushing test (Figure 6d–f and Supplementary Video S2) showed that the superhydrophobic copper foam could resist considerable water flow without failure as indicated by WCA measurements, where no decrease was observed. The coating remained intact without any detachment. Maximum water flow was calculated to be 0.03×10^{-6} m^3/s. The highest velocity of the water was 0.75 m/s.

Figure 6g–i depicts a modified copper foam sheet (with a diameter of 15 mm) which was placed into a beaker with water and engine oil droplets. The superhydrophobic copper foam surface could easily absorb oil molecules due to its sticky force. The absorption capacity amounted to 6 times the weight of the copper foam itself.

3.3. Oil-Water Separation

To estimate the oil/water separation efficiency, the optimum superhydrophobic coated copper foam (having the highest WCA) was chosen for all cases examined. A two section rectangular small tank (Figure 7a) was employed. It was filled with 60 mL of water and 20 mL of various engine oils. Two-stroke engine oil (ENO1) has the lowest viscosity and car engine oil 20W-50 (ENO3) is the thickest of the three.

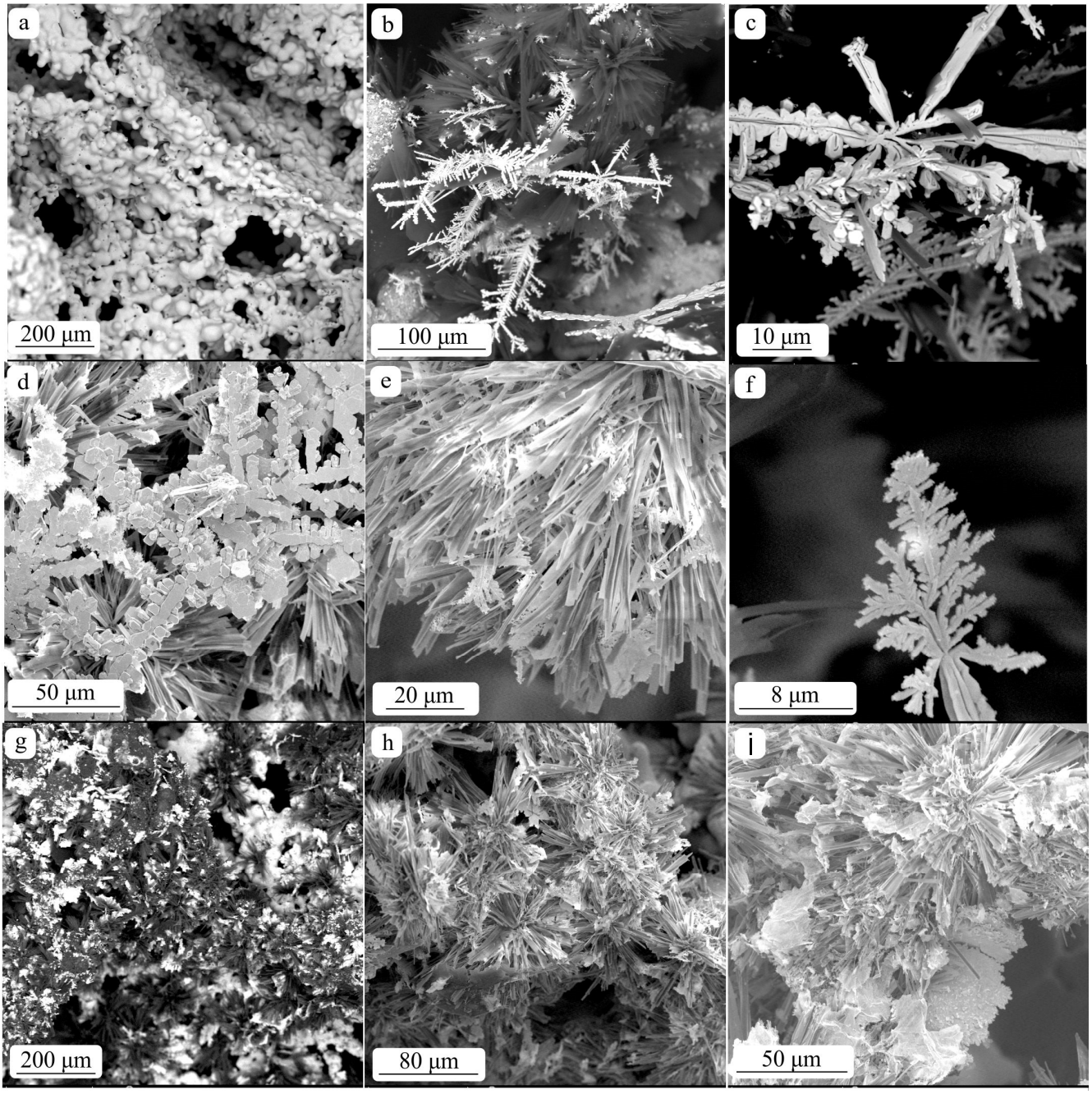

Figure 5. (**a**) Copper substrate. SEM images of hydrophobic films grown at: 20 min immersion time in silver nitrate solution and (**b**,**c**) 40 min in stearic acid solution, (**d**–**f**) 50 min in stearic acid solution, (**g**–**i**) 60 min in stearic acid solution.

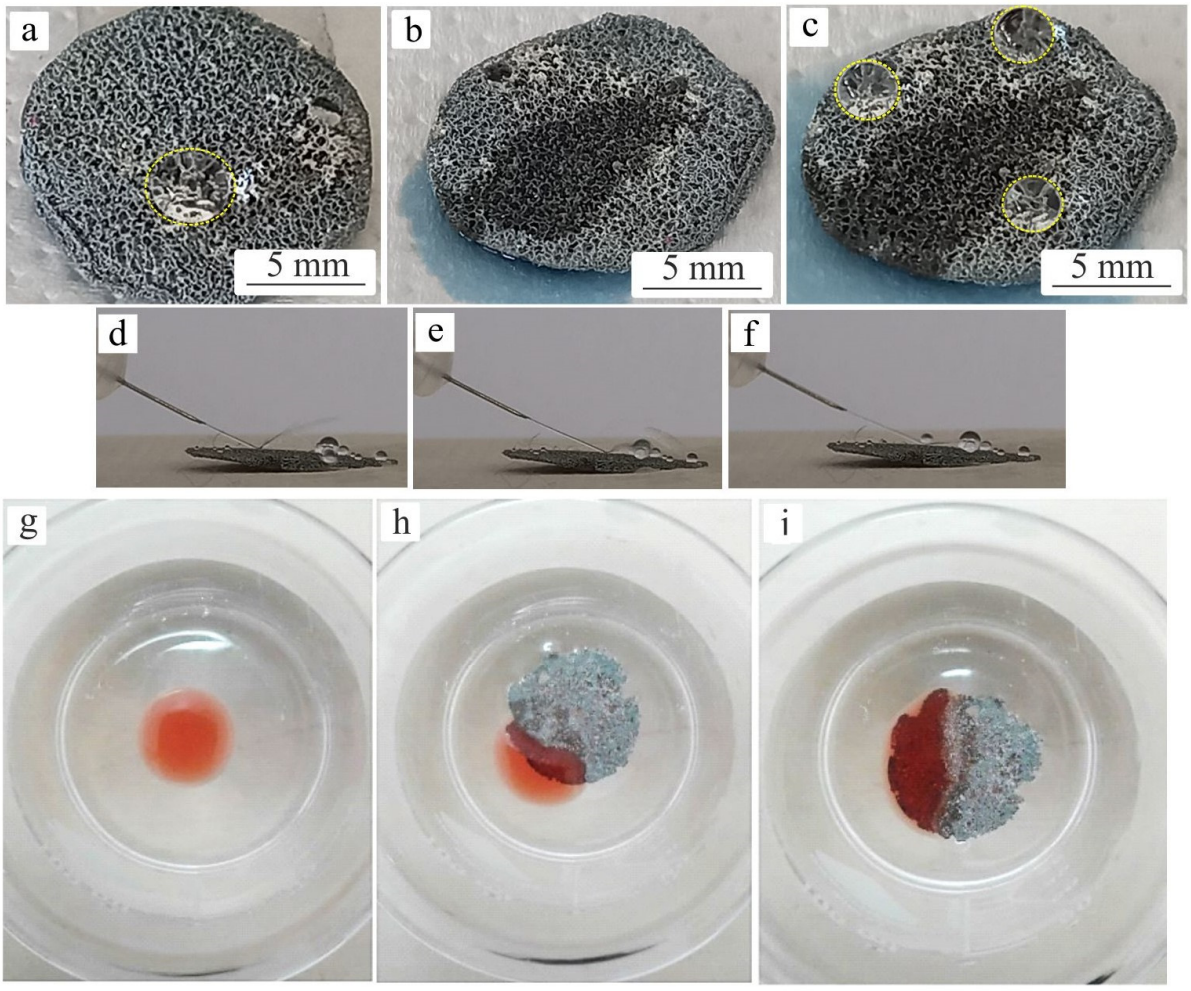

Figure 6. (**a**–**c**) Oil and water droplets, (**d**–**f**) continuous needle flushing test and (**g**–**i**) oil absorption test using a superhydrophobic copper foam.

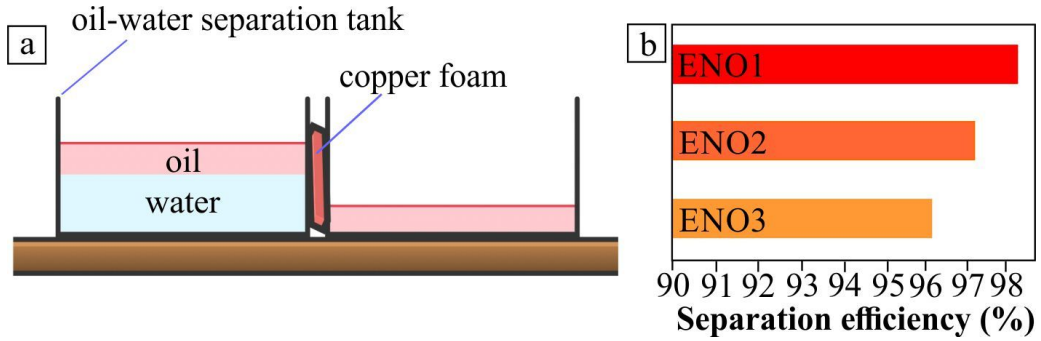

Figure 7. (**a**) Oil/water separation process, (**b**) separation efficiency for different engine oils.

Separation efficiency of the superhydrophobic copper foams depends on the oil's viscosity. Figure 7b shows separation efficiency of the coated samples for the three types of oil. The highest separation efficiency was achieved with the ENO1. Overall, the modified samples showed excellent separation efficiency above 95% in all tested cases.

3.4. Thermal and Chemical Stability

To assess the superhydrophobic copper foam durability under thermal loads, the modified copper foam samples were placed into a laboratory incubator at 100 °C and into a cooling chamber at −15 °C, for 1 h and 3 h. Figure 8a shows WCA measurements

after these thermal treatments. In both temperatures, the WCA decreased but the foam remained hydrophobic. In Figure 8b–d, the superhydrophobic coating's morphology after 1 h in −15 °C is depicted. The leaf-like morphology is partially disintegrated since the Ag leaf-like structures seem to consolidate with each other and are joined together (Figure 8c) or even destroyed leaving only the central nanoribbon of the leaf (Figure 8d), thus leading to partial loss of the copper foam hydrophobicity.

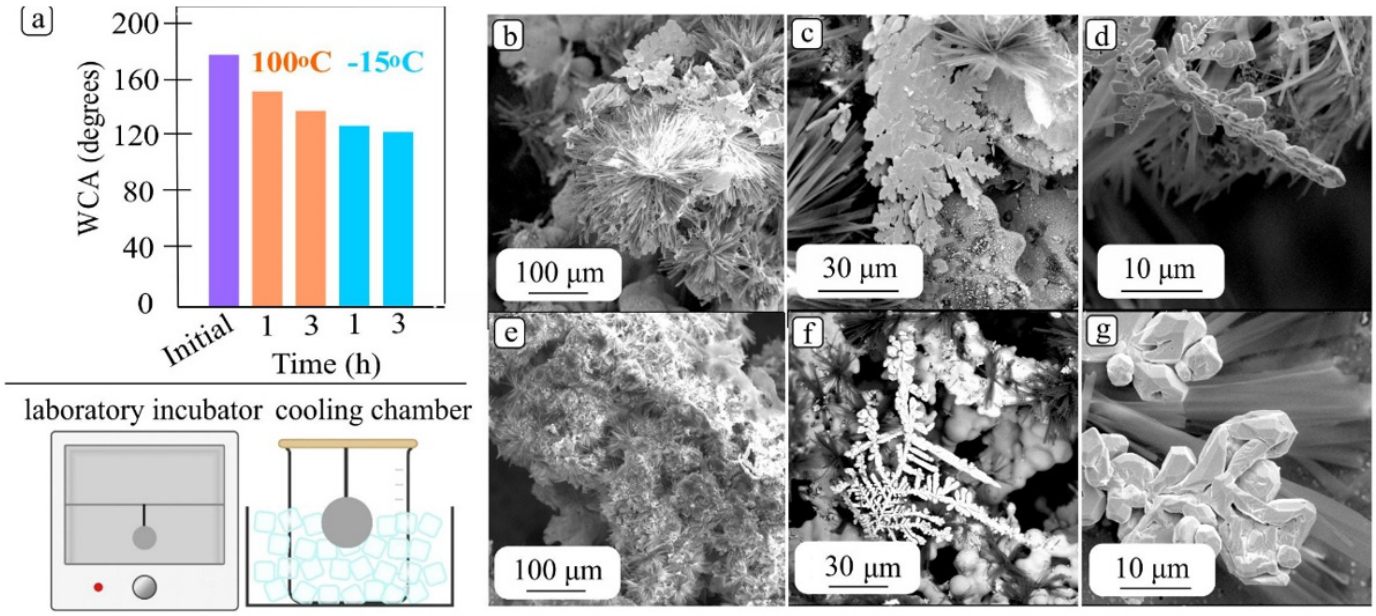

Figure 8. (**a**) WCA measurements after thermal treatment in 100 °C and −15 °C. SEM images of morphologies after thermal treatment (**b**–**d**) after 1 h in −15 °C, (**e**–**g**) after 1 h in 100 °C.

SEM images of modified copper foam morphology, Figure 8e–g, after 1 h residence time in 100 °C revealed a degradation of the leaf-like structure for the Ag. In Figure 8g, the destruction of the two-tier roughness is depicted whilst the copper stearic micro-clusters seem to be slightly "melted" and consolidated with each other.

Superhydrophobic copper foam's durability was also tested in acidic and alkaline solutions. Samples were immersed into HCl and NaOH solutions, for 1 h and 3 h. The values of WCA after chemical treatments are depicted in Figure 9a. SEM images of morphologies (Figure 9b) after 1 h in HCl solution reveal an aggregation of leaf-like and spherical structures. Higher magnification SEM images reveal the fracture of the silver fractal microstructure. In Figure 9c, the surfaces' structure after 1 h residence time in NaOH solution is depicted. A less extensive microstructural destruction was observed. Copper stearic micro-flowers remained almost intact and the silver leaf-like morphology presented high stability in alkaline pH values, thus a small alteration in the hydrophobicity was recorded.

It should be mentioned that the thermal and chemical stability of the modified copper foam samples remain even when the samples are exposed for 24 h at −15 °C and 100 °C and in NaOH and HCl solutions. More specifically, the WCA measured after 24 h of immersion in NaOH and HCl solutions was retained, almost the same as with that obtained after 3 h of immersion for each case tested, respectively. The same applies for the thermal treatment, e.g., thermal treatment for 24 h, at both temperatures tested, does not provoke any additional decrement of the WCA, but the value remains stable and the same as those obtained for 3 h thermal treatment for each case tested, respectively. This extended exposure duration of 24 h indicates that the modified copper foams present satisfactory thermal and chemical stability.

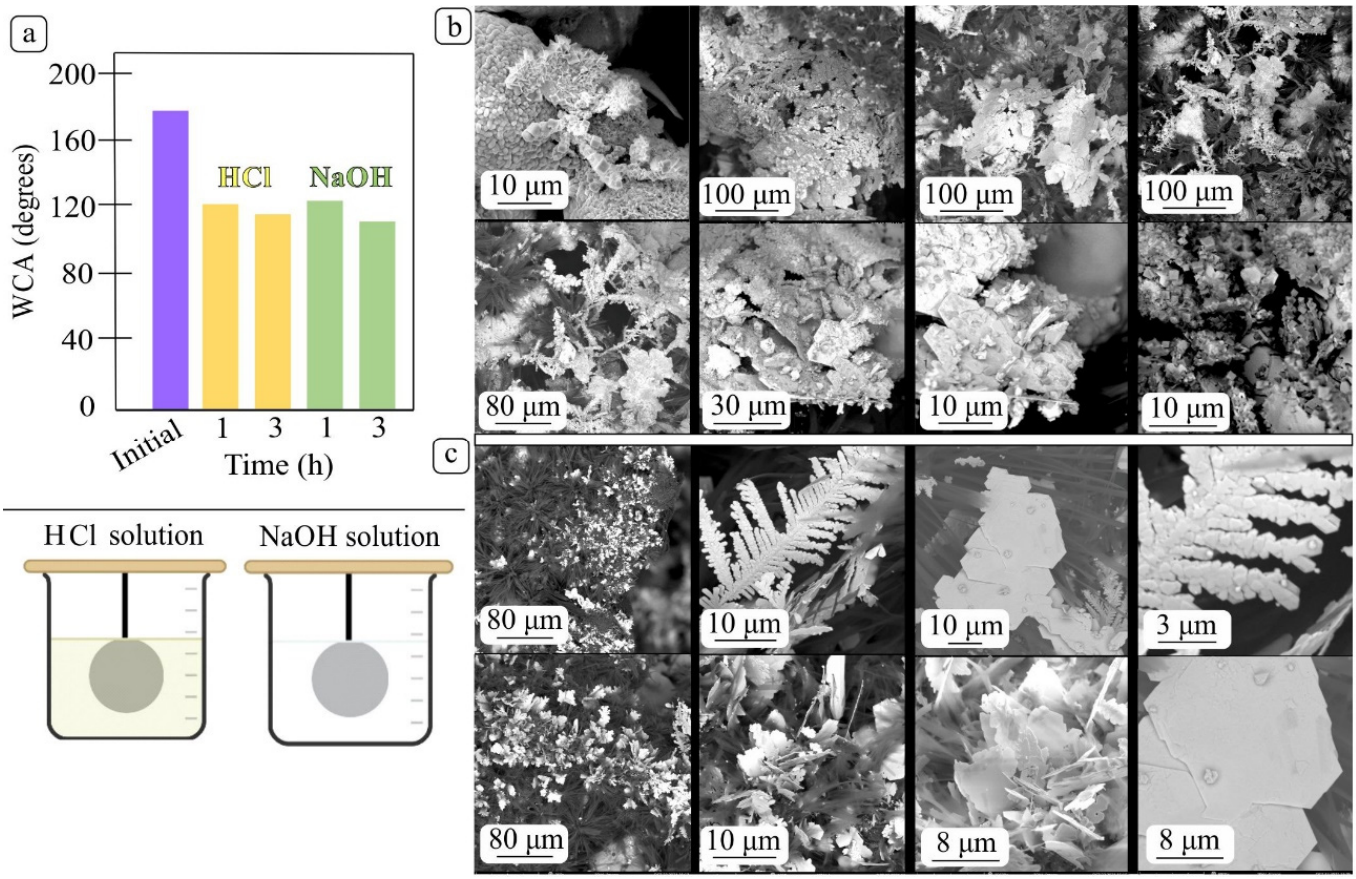

Figure 9. (**a**) WCA measurements after chemical treatment in acidic and alkaline solutions. SEM images of morphologies after (**b**) after 1 h in HCl solution, (**c**) after 1 h in NaOH solution.

4. Discussion

It is well documented that surface roughness asperities can lead to enhanced superhydrophobic properties of materials [52]. Several models are proposed to explain the surface roughness effect in the superhydrophobicity with the Wenzel and Cassie-Baxter being the most popular. Additional states are reported such as the lotus state, where the roughness asperities have also a nanostructured morphology [53].

The WCA of a non-modified copper foam ranges between 100° and 110°. However, this value can be misleading because the initial copper foams do not present any hydrophobicity. After 30 min, the 6 µL water droplets penetrate the foam (Figure 10a). This initial "apparent" hydrophobicity of the unmodified foam is ascribed to the inherent roughness asperities of the foam combined with the complex 3D pore structure of the foam (Figure 5a), which, however, are not sufficient for long-lasting hydrophobic properties. Moreover, if the unmodified copper foam is fully wet then the unmodified copper foam does not exhibit any hydrophobicity. The water droplets immediately flow through the foam, in that case (Figure 10a).

A high static contact angle along with low contact angle hysteresis and low sliding angle are desirable for efficient water repellency of a surface. The wetting repellency mechanism is schematically illustrated in Figure 10a,b for both pristine and modified copper foam. The produced modified copper foam exhibits a WCA of 180° and a sliding angle of 0° since the water droplet rolls immediately off the surface in horizontal position of the sample (Figure 10a). This excellent performance of the modified copper foam was attributed mainly to the extremely low contact area due to the complex and branched nano-/micro-morphologies developed, giving rise to nano-roughness asperities (Figure 4). The very fine developed nano- and micro-morphologies (either silver or copper stearate)

on the modified copper foam, depicted in Figure 4, lead to weak interaction of the two-tier roughness asperities with the water droplet and almost no sliding resistance. This is ascribed to the very low contact area which can be considered as a point contact area (Figure 10b), thus resulting to the highest WCA and lowest sliding angle. Additionally, the developed roughness asperities of the modified copper foam are tightly packed, which is reportedly favorable for water repellency, since this configuration could retain an interface air layer when in contact with water [52]. One the other hand, the pristine copper foam develops a higher contact area (face contact area in Figure 10b) which leads to a smaller interface air layer when in contact with a water droplet and lower WCA.

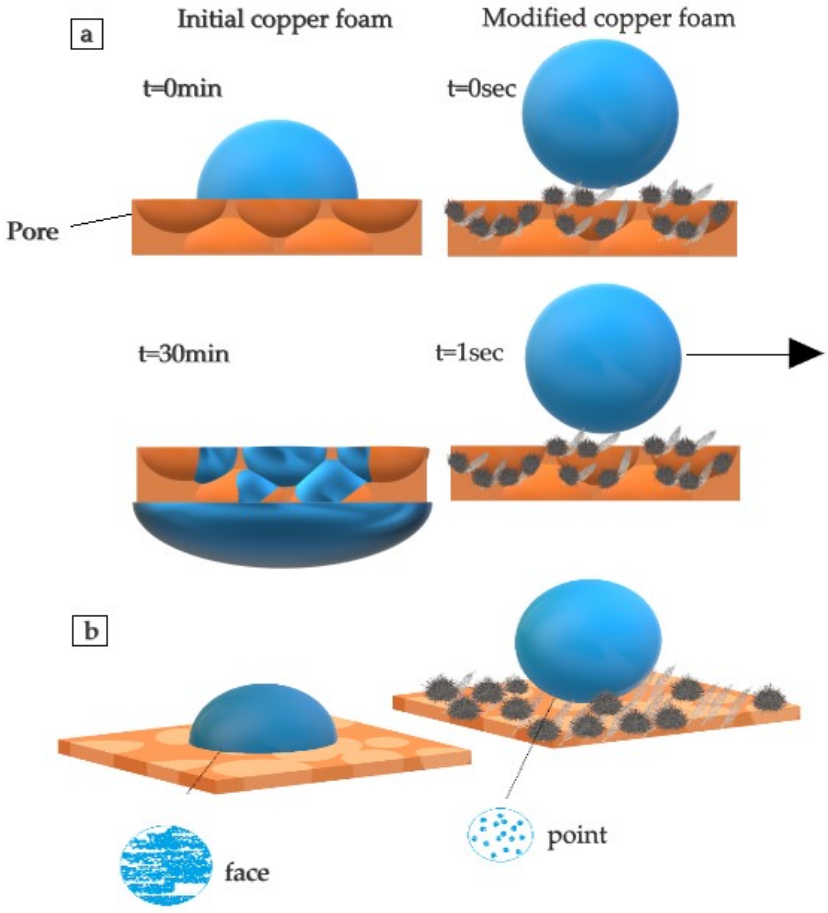

Figure 10. (**a**) Schematic diagram of wetting repellency mechanism (**b**) illustration of contact areas for a pristine (initial) and modified copper foam.

5. Conclusions

Superhydrophobic copper foams were successfully produced with a simple and effective method, based on chemical solutions. The optimum immersion durations were determined via UV-Vis and WCA measurements to 20 min in silver nitrate solution and 50 min in stearic solution. Such samples appear to have a 180 °C WCA and a dual morphology in their microstructure: a leaf-like one from the silver precipitation and microflowers morphology from copper stearic deposition. WCA measurements combined with SEM characterization demonstrated that the superhydrophobic copper foams possess high thermal and chemical stability under the examined acidic, alkaline and temperature conditions. Indicative oil absorption and separation tests of optimum produced superhydrophobic copper foams were satisfactory, which confirms their potential use as filters for oil treatment procedures.

Supplementary Materials: The following supporting information can be downloaded at: https://www.mdpi.com/article/10.3390/coatings13020355/s1, Video S1: Dynamic rolling test; Video S2: Continuous needle flushing test.

Author Contributions: Conceptualization, F.S. and A.B.; methodology, A.B.; validation, N.P.; formal analysis, A.B. and N.P. and L.M.; investigation, A.B., N.P. and L.M.; writing—original draft preparation, A.B. and F.S.; writing—review and editing, G.V., S.S. and F.S.; visualization, A.B.; supervision, F.S.; project administration, F.S. and S.S. All authors have read and agreed to the published version of the manuscript.

Funding: This research was funded by the Research Committee, Aristotle University of Thessaloniki, grant number 89251.

Institutional Review Board Statement: Not applicable.

Informed Consent Statement: Not applicable.

Data Availability Statement: Data is contained within the article and Supplementary Videos S1 and S2.

Conflicts of Interest: The authors declare no conflict of interest.

References

1. Mu, L.; Yue, X.; Hao, B.; Wang, R.; Ma, P.C. Facile preparation of melamine foam with superhydrophobic performance and its system integration with prototype equipment for the clean-up of oil spills on water surface. *Sci. Total Environ.* **2022**, *833*, 155184. [CrossRef] [PubMed]
2. Li, J.; Gao, R.; Wang, Y.; Zhang, T.C.; Yuan, S. Superhydrophobic palmitic acid modified $Cu(OH)_2$/CuS nanocomposite-coated copper foam for efficient separation of oily wastewater. *Colloids Surf. A Physicochem. Eng. Asp.* **2022**, *637*, 128249. [CrossRef]
3. An, K.; Zhang, X.; Qing, Y.; Long, C.; Sui, Y.; Yang, Z.; Wang, L.; Liu, C. One-step fabrication of robust superhydrophobic cerium-based nickel foam for oil-water separation and photocatalytic degradation. *J. Taiwan Inst. Chem. Eng.* **2021**, *129*, 246–255. [CrossRef]
4. Shi, Y.; Zhong, Y.; Sun, Z.; Ma, X.; Li, S.; Wang, F.; An, Y.; Luo, Q.; Zhu, J.; Chen, J.; et al. One-step foam assisted synthesis of robust superhydrophobic lignin-based magnetic foams for highly efficient oil-water separation and rapid solar-driven heavy oil removal. *J. Water Process Eng.* **2022**, *46*, 102643. [CrossRef]
5. Xue, Y.; Duan, S.; Du, T.; Hongkun, Y.C.; Li, M.; Chen, J. Facile synthesis of superwetting FeNi foam for oil/water separation. *Colloids Surf. A Physicochem. Eng. Asp.* **2022**, *636*, 128152. [CrossRef]
6. Sui, W.; Hu, H.; Lin, Y.; Yi, P.; Miao, L.; Zhang, H.; He, H.; Li, G. Mussel-inspired pH-responsive copper foam with switchable wettability for bidirectional oil-water separation. *Colloids Surf. A Physicochem. Eng. Asp.* **2021**, *630*, 127603. [CrossRef]
7. Chen, Z.; Zuo, J.; Zhao, T.; Tan, Q.; Nong, Y.; Xu, S.; Cheng, J.; Wen, X.; Pi, P. Superhydrophobic copper foam bed with extended permeation channels for water-in-oil emulsion separation with high efficiency and flux. *J. Environ. Chem. Eng.* **2023**, *11*, 109018. [CrossRef]
8. Wang, Y.; Ou, B.; Zhu, P.; Niu, B.; Gu, Y.; Zhi, Q. High mechanical strength aluminum foam epoxy resin composite material with superhydrophobic, anticorrosive and wear-resistant surface. *Surf. Interfaces* **2022**, *29*, 101747. [CrossRef]
9. Liu, H.; Zhai, W.; Park, C.B. Biomimetic hydrophobic plastic foams with aligned channels for rapid oil absorption. *J. Hazard. Mater.* **2022**, *437*, 129346. [CrossRef]
10. Bharat, B. Bioinspired oil–water separation approaches for oil spill clean-up and water purification. *Phil. Trans. R. Soc. A* **2019**, *377*, 20190120. [CrossRef]
11. Zhao, G.; Li, J.; Huang, Y.; Yang, L.; Ye, Y.; Walsh, F.C.; Chen, J.; Wang, S. Robust Ni/WC superhydrophobic surfaces by Electrodeposition. *RSC Adv.* **2017**, *7*, 44896–44903. [CrossRef]
12. Luo, Z.-Y.; Chen, K.-X.; Wang, J.-H.; Mo, D.-C.; Lyu, S.-S. Hierarchical nanoparticle-induced superhydrophilic and under-water superoleophobic Cu foam with ultrahigh water permeability for effective oil/water separation. *J. Mater. Chem. A* **2016**, *4*, 10566–10574. [CrossRef]
13. Wang, Z.; Yang, H.-C.; He, F.; Peng, S.; Li, Y.; Shao, L.; Darling, S.B. Mussel-Inspired Surface Engineering for Water-Remediation Materials. *Matter* **2019**, *1*, 115–155. [CrossRef]
14. Zhang, Y.; Liu, J.; Quyang, L.; Li, J.; Xie, G.; Yan, Y.; Weng, C. One-Step Preparation of Robust Superhydrophobic Foam for Oil/Water Separation by Pulse Electrodeposition. *Langmuir* **2021**, *37*, 7043–7054. [CrossRef] [PubMed]
15. Hu, Y.; Zhu, Y.; Wang, H.; Wang, C.; Li, H.; Zhang, X.; Yuan, R.; Zhao, Y. Facile preparation of superhydrophobic metal foam for durable and high efficient continuous oil-water separation. *Chem. Eng. J.* **2017**, *322*, 157–166. [CrossRef]
16. Ji, K.; Liu, J.; Zhang, J.; Chen, J.; Dai, Z. Super-floatable multidimensional porous metal foam integrated with a bionic superhydrophobic surface. *J. Mater. Chem. A* **2014**, *2*, 16589–16593. [CrossRef]
17. Zhang, Z.; Zhang, P.; Gao, Y.; Yun, J. Fabrication of superhydrophobic copper meshes via simply soaking for oil/water separation. *Colloids Surf. A Physicochem. Eng. Asp.* **2022**, *642*, 128648. [CrossRef]

18. Xia, L.; Chen, F.; Cai, Z.; Chao, J.; Tian, Y.; Zhang, D. Magnet-Assisted Selective Oil Removal from Water in Non-Open Channel and Continuous Oil Spills Clean-Up. *Sep. Purif. Technol. Part B* **2022**, *282*, 120119. [CrossRef]
19. Cao, Z.; Ouyang, Z.; Liu, Z.; Li, Y.; Ouyang, Y.; Lin, J.; Xie, X.; Long, J. Effects of surface oxides and nanostructures on the spontaneous wettability transition of laser-textured copper surfaces. *Appl. Surf. Sci.* **2021**, *560*, 150021. [CrossRef]
20. Du, J.; Chen, L.; Zeng, X.; Yu, S.; Zhou, W.; Tan, L.; Dong, L.; Zhou, C.; Cheng, J. Hard-and-Soft Integration Strategy for Preparation of Exceptionally Stable Zr(Hf)-UiO-66 via Thiol–Ene Click Chemistry. *ACS Appl. Mater. Interfaces* **2020**, *12*, 28576–28585. [CrossRef]
21. Caldona, E.B.; Brown, H.O.; Smith, D.W., Jr.; Wipf, D.O. Superhydrophobic/Superoleophilic Surfaces by Electroless Nanoparticle Deposition and Perfluorinated Polymer Modification. *Ind. Eng. Chem. Res.* **2021**, *60*, 14239–14250. [CrossRef]
22. Caldona, E.B.; Sibaen, J.W.; Tactay, C.B.; Mendiola, S.L.D.; Abance, C.B.; Añes, M.P.; Serrano, F.D.; De Guzman, M.S. Preparation of spray-coated surfaces from green-formulated superhydrophobic coatings. *SN Appl. Sci.* **2019**, *1*, 1657. [CrossRef]
23. Zhang, J.; Chen, R.; Liu, J.; Liu, Q.; Yu, J.; Zhang, H.; Jing, X.; Zhang, M.; Wang, J. Construction of ZnO@Co_3O_4-loaded nickel foam with abrasion resistance and chemical stability for oil/water separation. *Surf. Coat. Technol.* **2019**, *357*, 244–251. [CrossRef]
24. Eum, K.Y.; Phiri, I.; Kim, J.W.; Choi, W.S.; Ko, J.; Myoun, K.; Jung, H. Superhydrophobic and superoleophilic nickel foam for oil/water separation. *Korean J. Chem. Eng.* **2019**, *36*, 1313–1320. [CrossRef]
25. Álvarez-Gil, L.; Ramírez, J.; Fernández-Morales, P. Ultra-hydrophobic aluminum foam development for potential application in continuous water-oil separation processes. *Surf. Interfaces* **2021**, *26*, 101362. [CrossRef]
26. Tang, F.; Wang, D.; Zhou, C.; Zeng, X.; Du, J.; Chen, L.; Zhou, W.; Lu, Z.; Tan, L.; Dong, L. Natural polyphenol chemistry inspired organic-inorganic composite coating decorated PVDF membrane for oil-in-water emulsions separation. *Mater. Res. Bull.* **2020**, *132*, 110995. [CrossRef]
27. Zeng, X.; Cai, W.; Fu, S.; Lin, X.; Lu, Q.; Liao, S.; Hu, H.; Zhang, M.; Zhou, C.; Wen, X.; et al. A novel Janus sponge fabricated by a green strategy for simultaneous separation of oil/water emulsions and dye contaminants. *J. Hazard. Mater. Part B* **2022**, *424*, 127543. [CrossRef]
28. Liu, Y.; Zhan, B.; Zhang, K.; Kaya, C.; Stegmaier, T.; Han, Z.; Ren, L. On-demand oil/water separation of 3D Fe foam by controllable wettability. *Chem. Eng. J.* **2018**, *331*, 278–289. [CrossRef]
29. Zhang, K.; Lia, H.; Yina, X.; Wang, Z. Oil/water separation on structure-controllable Cu mesh: Transition of superhydrophilic-superoleophilic to superhydrophobic-superoleophilic without chemical modification. *Surf. Coat. Technol.* **2019**, *358*, 416–426. [CrossRef]
30. Zhang, Y.-P.; Yang, J.-H.; Li, L.-L.; Cui, C.-X.; Li, Y.; Liu, S.-Q.; Zhou, X.-M.; Qu, L.-B. Facile Fabrication of Superhydrophobic Copper-Foam and Electrospinning Polystyrene Fiber for Combinational Oil–Water Separation. *Polymers* **2019**, *11*, 97. [CrossRef]
31. Xu, M.; Chen, Y.-F.; Liang, J.-Y.; Mo, D.-C.; Lyu, S.-S. Electrodeposition Patterned Copper Foam with Micro/Nanostructures for Reducing Supercooling in Water-Based Cool Storage Phase-Change Materials. *Appl. Sci.* **2020**, *10*, 4202. [CrossRef]
32. Rong, J.; Zhang, T.; Qiu, F.; Xu, J.; Zhu, Y.; Yang, D.; Dai, Y. Design and preparation of efficient, stable and superhydrophobic copper foam membrane for selective oil absorption and consecutive oil–water separation. *Mater. Des.* **2018**, *142*, 83–92. [CrossRef]
33. Xu, J.; Jinliang, X.; Cao, Y.; Ji, X.; Yan, Y. Fabrication of non-flaking, superhydrophobic surfaces using a one-step solution-immersion process on copper foams. *Appl. Surf. Sci.* **2013**, *286*, 220–227. [CrossRef]
34. Wang, Q.C.; Yang, X.D.; Shang, G.R. Fabrication of copper-based Superhydrophobic surface through template deposition. *Adv. Mater. Res.* **2014**, *915–916*, 799–802. [CrossRef]
35. Bhagat, S.D.; Gupta, M.C. Superhydrophobic microtextured polycarbonate surfaces. *Surf. Coat. Technol.* **2015**, *270*, 117–122. [CrossRef]
36. Shirazy, M.R.S.; Blais, S.; Fréchette, L.G. Mechanism of wettability transition in copper metal foams: From superhydrophilic to hydrophobic. *Appl. Surf. Sci.* **2012**, *258*, 6416–6424. [CrossRef]
37. Asif, R.; Khan, H.N.; Jomiur, N.A.; Haq, M.U. To Determine the Concentration of Cobalt (II) In The Cobalt (II) Nitrate Hexahydarate Solution by UV-Visible Spectroscopy. *J. Appl. Chem.* **2019**, *12*, 22–27.
38. Gu, Q.; Chen, Y.; Chen, D.; Zhang, Z. Construction of super-hydrophobic copper alloy surface by one-step mixed solution immersion method. *IOP Conf. Ser. Earth Environ. Sci.* **2018**, *108*, 022038. [CrossRef]
39. Stergioudi, F.; Baxevani, A.; Mavropoulos, A.; Skordaris, G. Deposition of Super-Hydrophobic Silver Film on Copper Substrate and Evaluation of Its Corrosion Properties. *Coatings* **2021**, *11*, 1299. [CrossRef]
40. Nakamura, T.; Magara, H.; Herbani, Y.; Sato, S. Fabrication of silver nanoparticles by highly intense laser irradiation of aqueous solution. *Appl. Phys. A Mater. Sci. Process.* **2011**, *104*, 1021–1024. [CrossRef]
41. Rodríguez-León, E.; Iñiguez-Palomares, R.; Navarro, R.E.; Herrera-Urbina, R.; Tánori, J.; Iñiguez-Palomares, C.; Maldonado, A. Synthesis of silver nanoparticles using reducing agents obtained from natural sources (Rumex hymenosepalus extracts). *Nanoscale Res. Lett.* **2013**, *8*, 318. [CrossRef] [PubMed]
42. Li, H.; Lu, Y.; Zou, X.; Wang, C.; Wei, H. One Step Preparation of Superhydrophobic Surface on Copper Substrate with Anti-Corrosion and Anti-Icing Performance. *Int. J. Electrochem. Sci.* **2020**, *15*, 10674–10683. [CrossRef]
43. Bakirdere, S.; Yilmaz, M.T.; Tornuk, F.; Keyf, S.; Yilmaz, A.; Sagdic, O.; Kocabas, B. Molecular characterization of silver-stearate nanoparticles (AgStNPs): A hydrophobic and antimicrobial material against foodborne pathogens. *Food Res. Int.* **2015**, *76*, 439–448. [CrossRef] [PubMed]
44. Hu, Z.-S.; Hsu, S.M.; Wang, P.S. Tribochemical and thermochemical reactions of stearic acid on copper surfaces studied by infrared microspectroscopy. *Tribol. Trans.* **1992**, *35*, 189–193. [CrossRef]

45. Dong, J.; McCormick, A.V.; Davis, H.T.; Whitcomb, D.R. Cation-Controlled Crystal Growth of Silver Stearate: Cryo-TEM Investigation of Lithium vs. Sodium Stearate. *Langmuir* **2010**, *26*, 2263–2267. [CrossRef]
46. Qu, L.; Dai, L. Novel silver nanostructures from silver mirror reaction on reactive substrates. *J. Phys. Chem. B* **2005**, *109*, 13985–13990. [CrossRef]
47. Che, P.; Liu, W.; Chang, X.; Wang, A.; Han, Y. Multifunctional silver film with superhydrophobic and antibacterial properties. *Nano Res.* **2016**, *9*, 442–450. [CrossRef]
48. Mdluli, S.; Revaprasadu, N. Time dependant evolution of silver nanodendrites. *Mater. Lett.* **2009**, *63*, 447–450. [CrossRef]
49. Li, H.; Sun, Y.; Wang, Z.; Wang, S. Constructing Superhydrophobic Surface on Copper Substrate with Dealloying-Forming and Solution-Immersion Method. *Materials* **2022**, *15*, 4816. [CrossRef]
50. Sui, S.; Quan, H.; Hu, Y.; Hou, M.; Guo, S. A strategy of heterogeneous polyurethane-based sponge for water purification: Combination of superhydrophobicity and photocatalysis to conduct oil/water separation and dyes degradation. *J. Colloid Interface Sci.* **2021**, *589*, 275–285. [CrossRef]
51. Wang, Y.; Zhao, S.; Guo, Z.; Huang, J.; Liu, W. Multi-layer superhydrophobic nickel foam (NF) composite for highly efficient water-in-oil emulsion separation. *Colloids Surf. A Physicochem. Eng. Asp.* **2021**, *628*, 127299. [CrossRef]
52. Nosonovsky, M.; Bhushan, B. Roughness optimization for biomimetic superhydrophobic surfaces. *Microsyst. Technol.* **2005**, *11*, 535–549. [CrossRef]
53. Wang, S.; Jiang, L. Definition of superhydrophobic states. *Adv. Mater.* **2007**, *19*, 3423–3424. [CrossRef]